Baltic Sea Region
Programme 2007-2013
Part-financed by the European Union
(European Regional Development Fund
and European Neighbourhood and
Partnership Instrument)

CHEMSEA
CHEMICAL MUNITIONS
SEARCH & ASSESSMENT

# Report of the magnetometric survey in the area of the Deep of Gdansk

| **Report 467/12** | **Date: 2012-05-15** **Version: 1.01** |
| --- | --- |
| Elaboration: | Agnieszka Brzezińska, Dorota Cichowska, Łukasz Gajewski, Wojciech Konieczny, Maria Kubacka, Jarosław Nowak |
| Correction: | Lucjan Gajewski |
| Approval: | Benedykt Hac |

Employee:

**Zakład Oceanografii Operacyjnej**
**Instytut Morski w Gdańsku**
**ul. Długi Targ 41/42**
**80-830 Gdańsk**

Employer:

**Akademia Marynarki Wojennej im. Bohaterów Westerplatte**
**ul. Śmidowicza 69**
**81- 103 Gdynia**

**May 2012, Gdańsk**

## Content



# 1 Aim of the survey

The aim of the survey was to collect and analyze the magnetometric data in the probable area of munitions dumping in Gdańsk Deep. The objects searched for, are chemical munitions dumped in the Baltic Sea in containers of ferromagnetic character. The estimated size of dumped containers (used to store the ammunition) is in line with the 150 mm artillery shells and with bulk containers in the shape of steel barrels. The main aim of magnetometric survey is to find a correlations between the geographical positions of objects that have been localized on seabed during the hydroacoustic survey and positions of Earth magnetic field disturbances in the area of Gdańsk Deep.

# 2 Legal basis

The legal basis of project accomplishment is the Contract nr 1/AMW/2012/NB dated February 27, 2012, annexed by Annex Contract nr 1 dated April 16, 2012 signed between Polish Naval Academy (PNA) as an employer and Maritime Institute in Gdańsk as an employee.

# 3 Geodetic basis

Coordinate system parameters used during the project conduct:

| | |
|---|---|
| **Parameters of the ellipsoid** | |
| Ellipsoid: | WGS 1984 |
| Coordinates system: | WGS84 |
| Main axle: | 6378137 |
| Flattening (1/f): | 1/298.2572236 |
| **Projection parameters** | |
| Projection: | Gauss-Krüger |
| Base Latitude: | 0˚ |
| Centre Meridian: | 19˚ E |
| Scale factor: | 0.9993 |
| False Northing: | -5 300 000 m |
| False Easting: | 500 000 m |

# 4 Measuring equipment

## 4.1 Measuring vessel

All the maritime surveys conducted under the order were carried out by the research vessel of Maritime Institute in Gdańk - R/V IMOR (Fig. 4.1.).

| | | |
|---|---|---|
| Vessel: | Callsign: | SNKB |
| | MMSI Number: | 2613 79 000 |
| | IMO Number: | IMO 9212565 |
| Technical data: | Length: | 32,50 m |
| | Width: | 10,50 m |
| | Draft: | 2,41 m |
| | Displacement: | 327 t |


*4.1. Research vessel of the Maritime Institute in Gdańsk – R/V „IMOR”*

Maximum speed: - 9 knots

Maximum weather conditions for acoustic surveying (seismic surveys):
- wind: 10 m/s,
- wave height: up to 1m.

Maximum weather conditions for bottom sediments sampling
- wind: 10 m/s,
- wave height: up to 1,5m.

Weather limitations and durability determined by the ship's class are: area A1 + A2 GMDSS and 200 NM from the shelter with winds up to 8º B and sea state up to 5º B.

## 4.2 Navigation system

The positioning of onboard sensors of IMOR (transceivers of echosounder and magnetometer) has been provided by a satellite positioning system DGPS AgGPS 132 (Fig. 4.2.) and RTK TRIMBLE SPS 851. Positioning corrections have been implemented with use of satellite system OMNISTAR. Position accuracy specified as double standard deviation (with confidence level 96%) was better than 2 meters. Positioning systems and sensors have been integrated within hydrographical integrated software QINSY v.8. The QINSY system allows to store all the measurements, to record all the parameters of the system, as well as to visualize the survey process, in order to enable the helmsman to steer precisely in accordance with planned survey lines.


*Fig. 4.2. Satellite positioning system AgGPS 132 of Trimble*

Given the known GPS antenna position and shifts of sensors' transceivers, the QINSY software converted in real-time coordinates of the antenna to rectangular coordinates of individual sensors.

The navigation system, that consisted of the navigation software QINSY v.8.0, has been gathering and recording the positioning data, motion sensor data (DMS), heading data (gyro) and the survey profile data. The results were transmitted in real time to the helmsman display and to the dynamic positioning system (DP), allowing to actively maintain the ship's position on the given survey line.

## 4.3 Magnetometric measuring device

The measurements of the Earth's magnetic field intensity have been conducted with utilization of a proton magnetometer SeaQuest of MarineMagnetics (Fig. 4.3.), configured to work with two additional magnetometric sensors and an altimeter. The sensitivity of the magnetometric sensors of SeaQuest magnetometer is 0,01 nT (nano Tesla), total accuracy of the magnetometer is 0,2 nT.

*Fig. 4.3. SeaQuest MarineMagnetics magnetometer*

# 5 Organizational structure of the project

## 5.1 Area and methods of work

During the measurements, the position of the magnetometer was determined by the underwater navigation system USBL SCOUT PRO. Therefore, the QINSY system recorded all the positions - the ship's position, the fish-mounted transponder's position and positions of three sensors of the magnetometer, found in SeaQuest device. The QINSY system allowed the calculation of all the actual positions of each of the sensors.

The values of magnetic induction were recorded on 56 profiles spaced at 10 m distance. The measurement data were stored in a QINSY standard format in files with the *.db extension. Upon the request of employer, the data was exported to the ASCII format files with the *.log extension – it will allow the employer to further process the data.


*Fig. 5.1. Location and arrangement of the measured polygon and test profiles during the measurements (http://www.marinetraffic.com)*

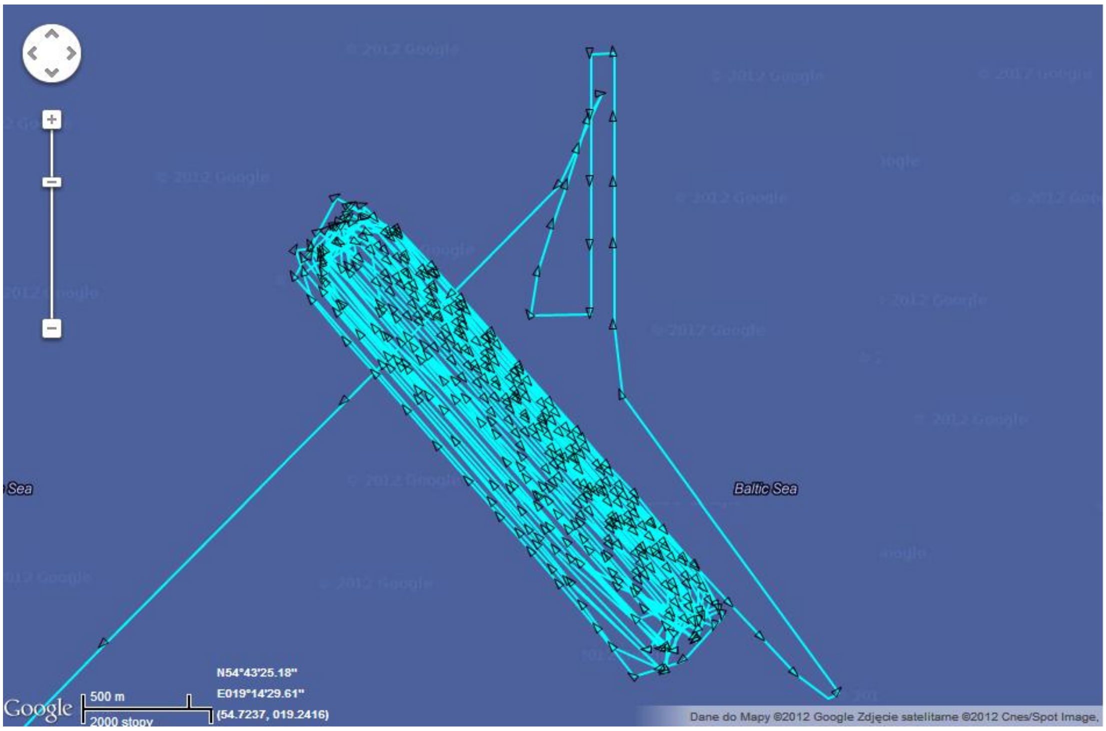


*Fig. 5.2. Location and arrangement of the measured polygon and test profiles during the measurements (http://www.marinetraffic.com)*

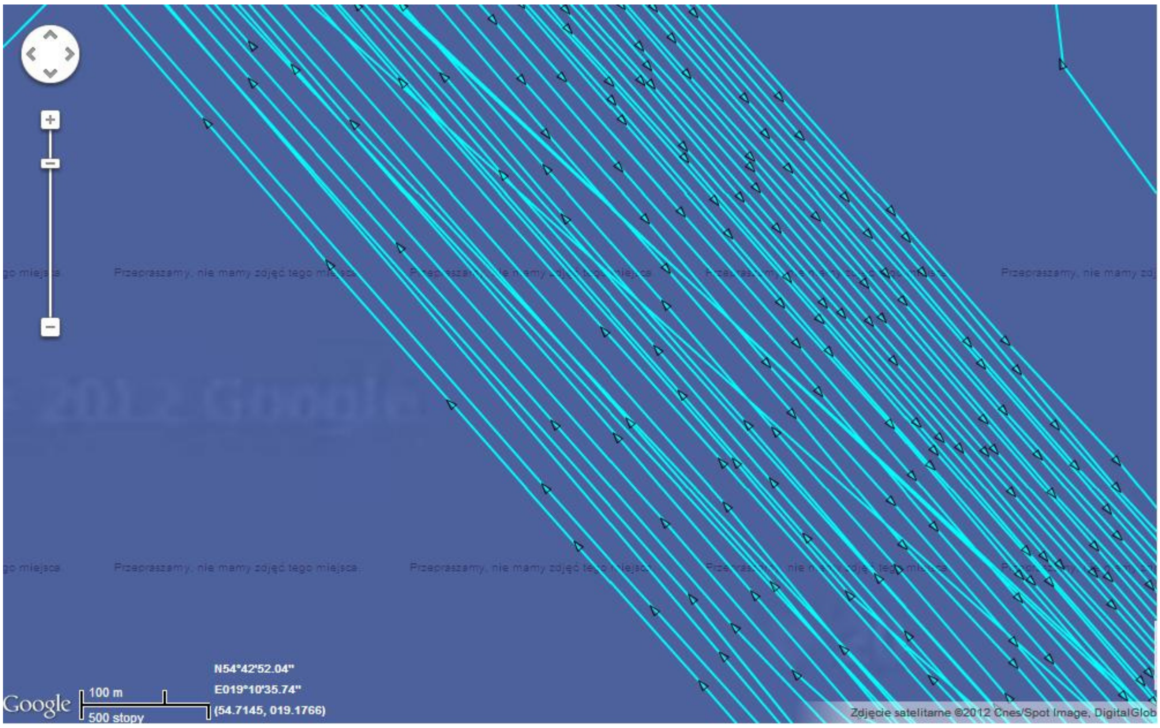


*Fig. 5.3. Distribution of measured profiles during the measurements (http://www.marinetraffic.com)*

## 5.2 Processing of collected data in order to identify ferromagnetic objects

The main purpose of magnetometric data processing is to detect local sources of the increased magnetic field intensity, indicating the presence of ferromagnetic objects in the area.

The data, containing the value of magnetic induction level recorded by the magnetometer, are difficult to interpret, mainly because it is characterized by the time and location dependences. In addition, the magnetic field intensity at any geographical point represents the sum of vectors of the natural magnetic field of the earth and, in case of presence of an object with ferromagnetic features, the vector of the object's magnetic dipole momentum.

The signal recorded by a magnetometer also includes noises that interfere the proper signal, which may be generated by the electrical devices (e.g. magnetometer itself, wire lines, vessel), the diurnal variations of the Earth's magnetic field caused by the Sun, measuring device self-noise, communication errors between the measuring device and recording system and noises generated by sea waves.

To reduce the above mentioned types of interferences, an initial low-pass signal filtering was carried out, to eliminate all the high frequency components. The next stage of the signal processing was the usage of low-pass Butterworth's filter characterized with maximum flat response function. The Butterworth's filter is a kind of filter with infinite impulse response operating in the time domain. This type of filtering does not require the usage of the Fourier's transformations and is, in general, about multiplication of samples by numbers, their delaying and summation. The main objective of the application of Butterworth's filter to the collected data was to eliminate the mean values, generated mainly by the Earth's magnetic field, and extraction of low-frequency components, indicating the presence of ferromagnetic objects.

The normalized data was used to develop magnetic anomaly map. Interpolation of filtered magnetometric data allows to present the magnetic field intensity values in the area of research site and to identify significant local anomalies, indicating the presence of ferromagnetic objects on the bottom or under a layer of sediments. Correlating the location of magnetic anomalies with magnetic sensors' distances from the sea bottom, along with the values registered by the sensors, makes it possible to determine the approximate weight of ferromagnetic object. The analysis of magnetic field intensity distribution maps also allows to specify the presence of larger geologic or geomorphologic forms.

Due to the high sensor response to changes of its height above the bottom, it is crucial to cautionary interpret the results, especially in qualifying individual dipoles as anomalies generated by ferromagnetics, rather than dipoles resulting from measurement errors, the variations of bathymetry or geomorphology of the bottom surface.

Sudden changes in depth of the area or in height of the sensor above the sea bottom provokes changes in actual value of the magnetic field intensity recorded by the device at a given point of space. This fact can be used, among others, to detect potential bottom thresholds or degree of differentiation of the seabed relief.

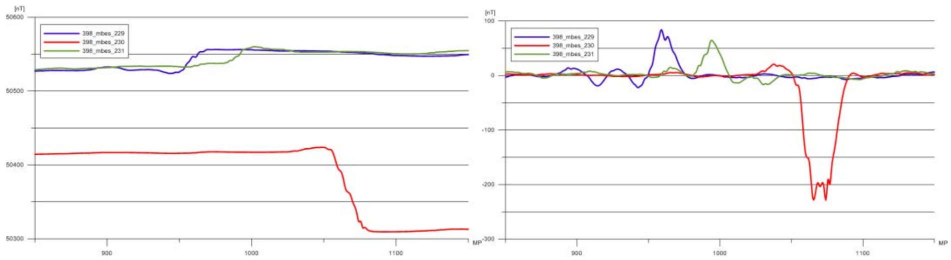


*Fig. 5.4. Examples of the magnetic field intensity recorded on 3 adjacent survey profiles, recorded during the previously made surveys (left) and data from the same profiles after filtering (right)*

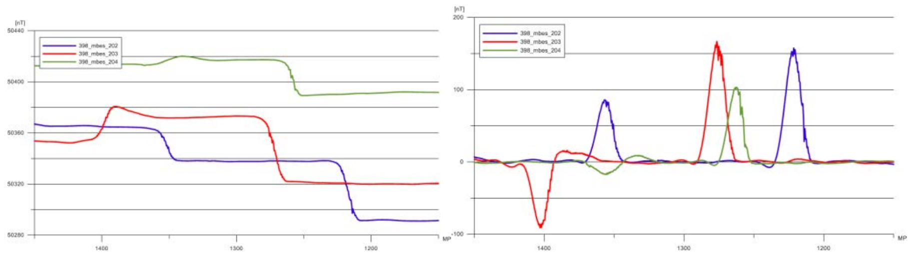


*Fig. 5.5. Examples of the magnetic field intensity recorded on 3 adjacent survey profiles, recorded during the previously made surveys (left) and data from the same profiles after filtering (right)*

The graphs (Fig. 5.4. and 5.5.) present the magnetic field intensity values recorded in another project at the sample survey line and the processed data output, generated with utilization of filtering method mentioned above.

The graphs representing the data before filtration (left) clearly depicts magnetic field intensity changes, which result from changes of depth in the area or from changes in the height of the measuring device above the sea bottom. As a result (right), the algorithm generates increased or significantly underestimated values of the magnetic field anomaly. This dependence can be used primarily to find boundaries of areas with different character, such as changes of the depth in the area.

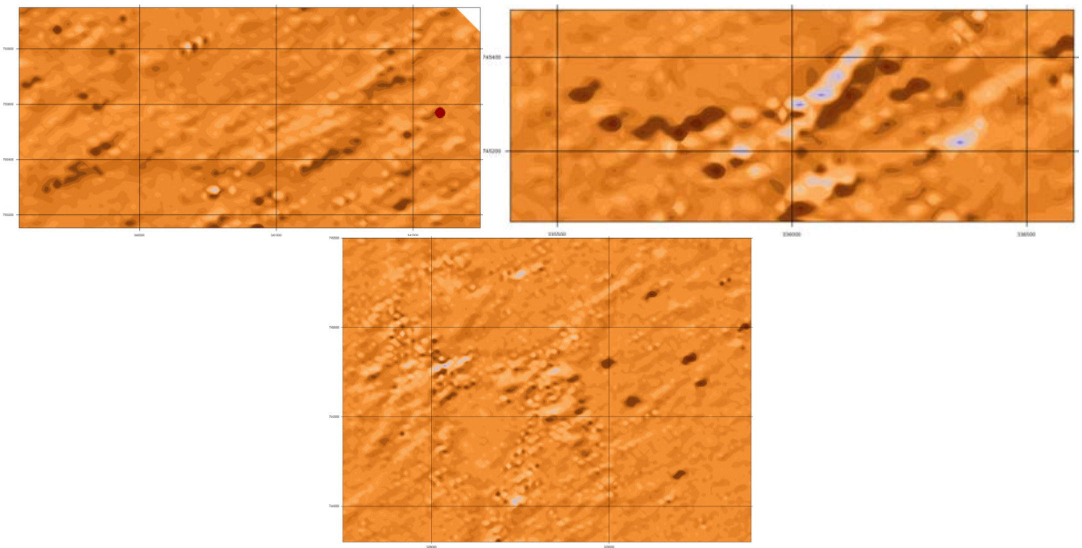

*Fig. 5.6. Examples of continuous magnetic anomaly indicating the existence of potential bottom thresholds or geomorphologic forms*

The illustrations (Fig. 5.6.) present fragments of the magnetic field anomalies map of the previously studied areas, with examples of continuous magnetic anomaly, which indicate the existence of bottom thresholds or occurrence of many different geomorphologic forms. The magnetometer device measures the ambient magnetic field intensity, which is affected by many factors, such as presence of ferromagnetic objects on the sea bottom or under a layer of sediments.

The intensity of the magnetic anomaly depends, among others, on the weight of ferromagnetic object and is approximately inversely proportional to the cube of the distance between measuring device and the object. This means, that the size of a ferromagnetic object that can be detected, is determined by the distance from the magnetometer to the object lying on the sea bottom. The two main parameters, that impact that distance are: the height, at which the measuring device is held above the sea bottom during the measurements and the distance between successive survey lines.

The most effective method of magnetometric measurements conducted in order to detect the number of objects on the sea bottom, is a dense arrangement of the survey profiles and keeping the magnetometer as close to the bottom as possible. Such conditions, however, cannot always be met. The bathymetry and natural conditions of the researched area are the main factors that affect the way the survey is carried out. Keeping the measuring device too close to the sea bottom, while conducting the survey in the area of variable bathymetry or diverse relief, creates a threat of hitting the bottom or dragging the device on the ground.

Dense deployment of measuring profiles increases the time and cost of the study period. In order to select the most optimal way of surveying, it is crucial to determine the smallest expected mass of objects that one wants to locate. The minimum value of the anomalies indicating the presence of a ferromagnetic object in the researched area is 5 nT. One also has to take into consideration, that small objects are detectable only at the survey line or at the short distance from the designated survey line, while only objects of a large mass can be detected in spaces between the survey lines. With the distribution of survey lines at the distance of 30 m and with a minimum distance of the magnetometer above the sea bottom of 6 m, any object with a mass of 0,5 t lying exactly between the survey lines generates an anomaly value of 1,2 nT, thus is not detected. The same object lying at the survey line will create an anomaly value of 24 nT (Hall 1966).

*Tab. 5.1. Examples of archaeological objects on the sea bottom and minimal distances between the measuring device and the target determining their detection (based on the Hall's equations, 1966)*

| Example of an object | Mass [kg] | Maximum distance from the magnetometer (anomaly 5 nT) |
|---|---|---|
| small gun | 9 kg | 2,7 m |
| medium gun | 14,5 kg | 3,1 m |
| small anchor | 100 kg | 5,9 m |
| medium anchor | 2 t | 15,9 m |
| steel wreck | 10 t | 27,1 m |
| steel wreck | 100 t | 58,4 m |
| steel wreck | 1000 t | 126 m |

The table above (Table 5.1.) shows, that small objects are difficult to detect. Within a distance of 6 m from the measuring device, none but objects weighting more than 100 kg will be perceived as an anomaly of 5 nT.

*Tab. 5.2. The minimum distances between a ferromagnetic object and a measuring device, assuming 5 nT detection (based on the Hall's equations 1966)*

| Distance (m) | Mass of an object (kg) |
|---|---|
| 5 | 63 |
| 6 | 108 |
| 7 | 172 |
| 8 | 256 |
| 9 | 365 |
| 10 | 500 |
| 12 | 864 |
| 14 | 1372 |
| 16 | 2048 |
| 18 | 2916 |
| 20 | 4000 |

*Fig. 5.7. Example of an object (torpedo weighing approximately 1.5 tons) on the sea bottom combined with the values of magnetic field anomalies*

The correctness of the used method is confirmed by the detection of small objects on the bottom, which presence is confirmed by the hydroacoustic images. The figure (Fig. 5.7.) shows an example of a torpedo sonar image with the superimposed contour lines of the magnetic field anomalies' values.

# 6 Results

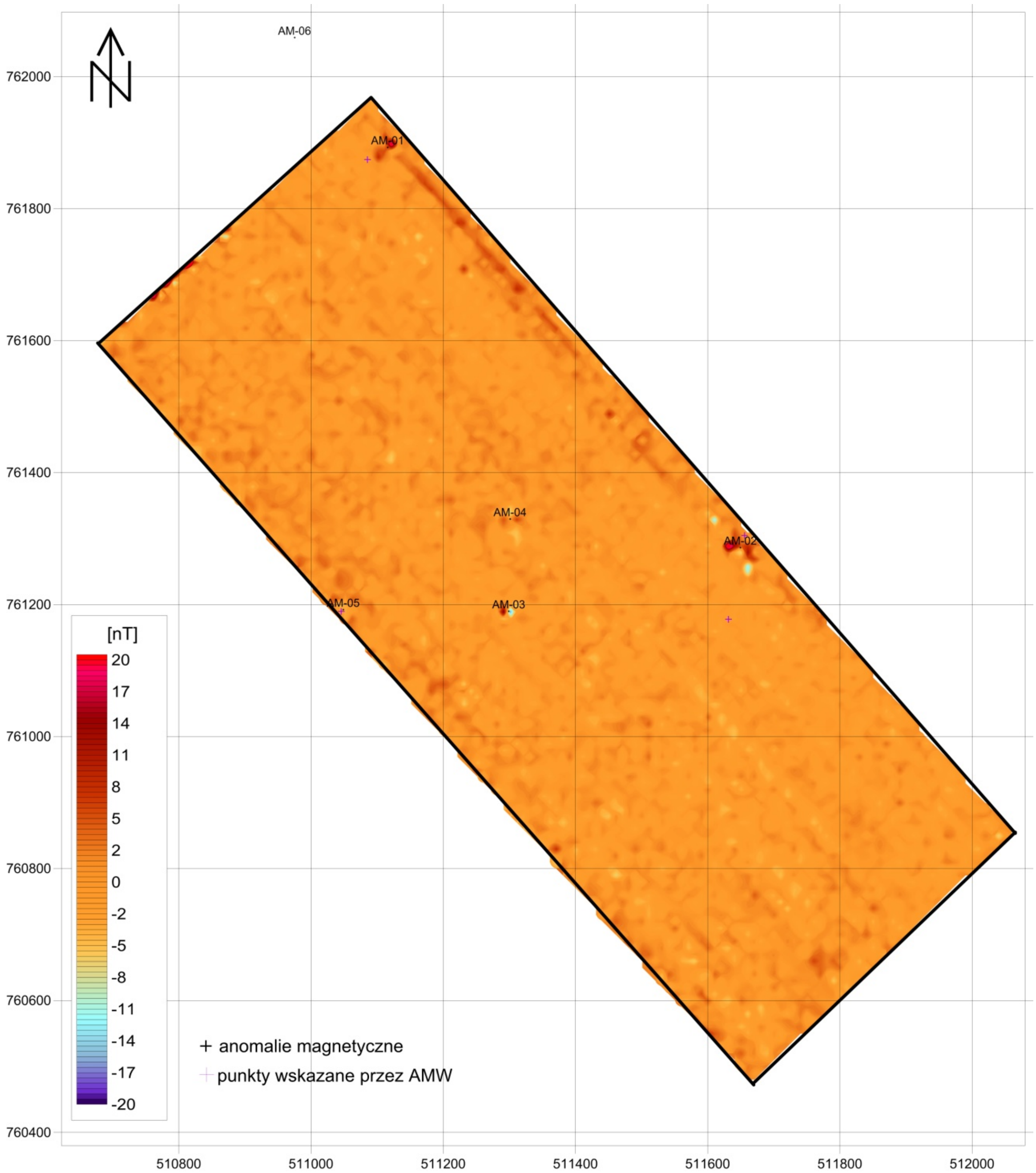


*Fig. 6.1. Map of the magnetic field anomalies distribution at the designated survey polygon*

The figure above (Fig. 6.1.) presents a distribution of magnetic anomalies at the designated survey polygon. The map shows the size of the magnetic field changes, while the colour scale determines their value. The visible constant magnetic anomalies point at the slight variations in the geomorphologic structure of the sea bottom. The areas with significantly higher values of magnetic field may designate the places of the depth change. The variability of the magnetic field distribution, which is visible on the map, may also be caused by different sediment types. For a thorough analysis and verification of the studied area, the magnetic anomaly map has to be compared with bathymetric and geological measurements.

In the survey area, there were determined 6 magnetic anomalies showing the presence of ferromagnetic object on the sea bottom or under a layer of sediment. The size of the magnetic anomaly depends on the mass of an object, its shape, spatial orientation and the material of which it is made, whereas the actual value detected by the sensor is further conditioned by the distance of the magnetometer from the sea bottom during the measurement and is approximately inversely proportional to the cube of the distance from the object to the device.

The table (Tab. 6.1.) shows combination of the magnetic anomalies detected during the research, their positions (Easting, Northing) and values of maximum magnetic field anomaly recorded by the sensor in the area. It should be noted, that the positions of magnetic anomalies on the map are only the closest approximation to the actual position of the object lying on the bottom, i.e. represent the situation, in which the magnetometer transited directly over the target.

*Tab. 6.1. List of magnetic anomalies identified in the surveyed area*

| Name of anomaly | Easting | Northing | Max value [nT] |
|---|---|---|---|
| AM-01 | 511115,9012 | 761892,9121 | 25 |
| AM-02 | 511649,4823 | 761286,2886 | 23 |
| AM-03 | 511299,1263 | 761189,724 | 15 |
| AM-04 | 511301,1376 | 761329,5029 | 8 |
| AM-05 | 511048,7087 | 761192,0776 | 5 |
| AM-06 | 510975,1499 | 762059,0554 | 40 |

A detailed magnetic anomalies intensity distribution for each object has been depicted on the enlarged fragments of the map of the magnetic field anomalies distribution.

## 6.1 Anomaly AM-01

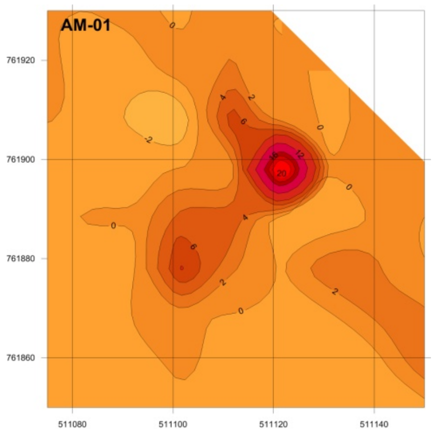


*Fig. 6.2. Enlarged map of the magnetic anomalies showing the anomaly AM-01 in detail*

In the figure above (Fig. 6.2.), there is presented a detailed distribution of the magnetic field for the anomaly AM-01. Values recorded by the sensor and spatial distribution of contour lines on the map show the occurrence of a ferromagnetic object in this region.

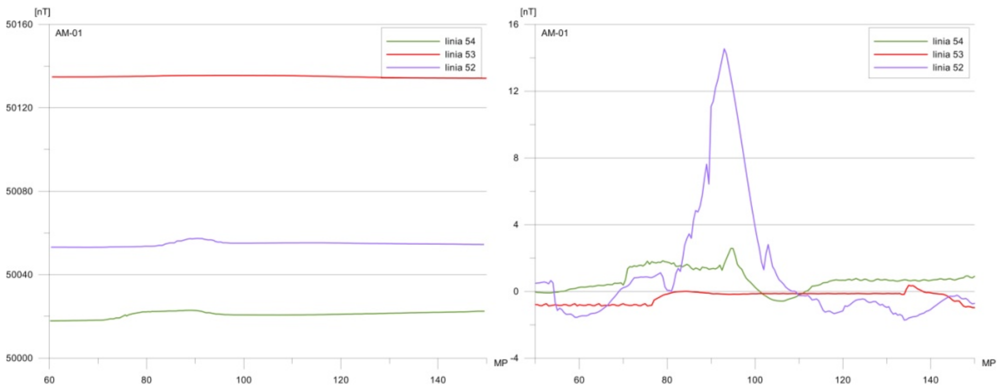


*Fig. 6.3. Charts of magnetic field intensity recorded by the measuring device in three adjoining measuring profiles at the site of the anomaly AM-01*

The figures (Fig. 6.3.) present the charts of a detailed magnetic field intensity distribution for the raw data recorded by the magnetometer on the measuring profiles *52 (the blue colour), 53 (the red colour), 54 (the green colour).* The charts on the right side represent the same data after the filtering process. On the profile 52, there is visible a clear magnetic anomaly of the value of 15 nT after the filtering process and signal normalization. The value recorded for the raw data is approximately 4 nT, which may indicate the presence of a ferromagnetic object in this region. On the adjoining measuring profiles no elevated magnetic fields intensity values have been recorded. The shape of the graph indicates a small distance between measuring device and the object during signal recording. It is also probable, that the object or a part of it is under a layer of sediments. It is likely, that the recorded signal may be a consequence of local variation of the bottom bathymetry or its construction.

## 6.2 Anomaly AM-02

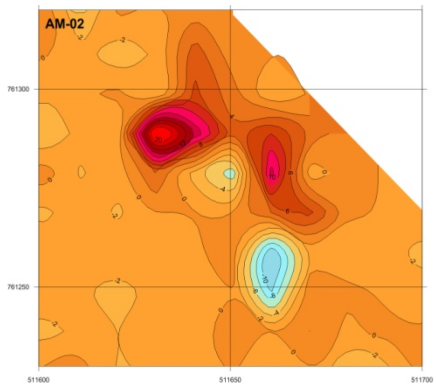


*Fig. 6.4. Enlarged map of the magnetic anomalies showing the anomaly AM-02 in detail*

The figure above (Fig. 6.4.) presents a detailed distribution of the magnetic field for the anomaly AM-02. Values recorded by the sensor and spatial distribution of contour lines on the map indicate the presence of a ferromagnetic object in this region.

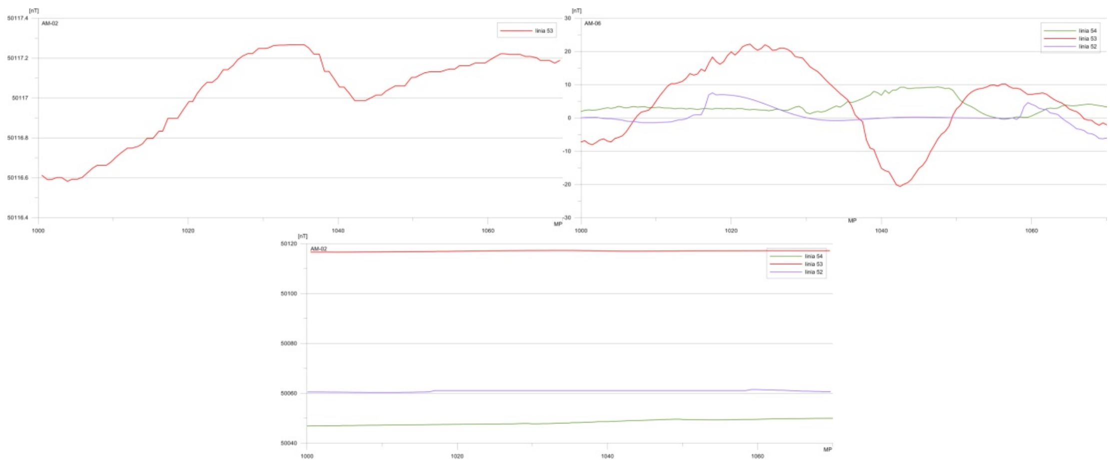

*Fig. 6.5. Charts of magnetic field intensity recorded by the measuring device on three adjoining measuring profiles at the site of the anomaly AM-02*

The figure (Fig. 6.5.) presents the charts of a detailed magnetic field intensity distribution for the raw data recorded by the magnetometer on the measuring profiles *52 (the blue colour), 53 (the red colour), 54 (the green colour).* The charts on the right side represent the same data after the filtering process. On the profile 52, there is visible a clear magnetic anomaly of the value of 20 nT after the filtering process and signal normalization. The value recorded for the raw data is approximately 6 nT, which may indicate the presence of a ferromagnetic object in this region. In addition, the increased value of the magnetic field was recorded at the adjoining measuring profiles, which may indicate an oblong shape of the object or its large size. The shape of the graph indicates a relatively large distance between the measuring device and object during the recording of the signal. It is also likely, that the object or its part is situated under a layer of sediments. The distribution of the recorded magnetic field is also influenced by the nature and shape of the bottom in the area.

## 6.3 Anomaly AM-03

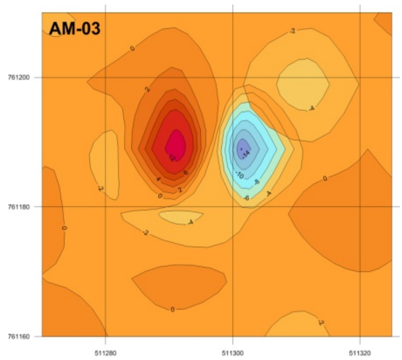


*Fig. 6.6. Enlarged map of the magnetic anomalies showing the anomaly AM-03 in detail*

The figure above (Fig. 6.6.) presents a detailed distribution of the magnetic field for the anomaly AM-03. Values recorded by the sensor and spatial distribution of contour lines on the map indicate the presence of a small ferromagnetic object in this region.

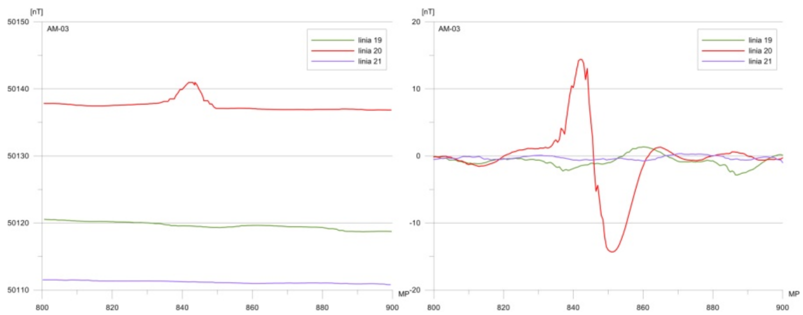


*Fig. 6.7. Charts of magnetic field intensity recorded by the measuring device on three adjoining measuring profiles at the site of anomaly AM-03*

The figures (Fig. 6.7.) presents charts of a detailed magnetic field intensity distribution for the raw data recorded by the magnetometer on the measuring profiles *19 (the blue colour), 20 (the red colour), 21 (the green colour).* The charts on the right side represent the same data after the filtering process. On the profile 20, there is visible a clear magnetic anomaly of the value of 15 nT after the filtering process and signal normalization. The value recorded for the raw data is approximately 3 nT, which may indicate the presence of a ferromagnetic object in this region. On the adjoining measuring profiles there have not been recorded any increase in magnetic field intensity. The shape of the graph indicates a relatively large distance between the measuring device and object during the signal recording. It is also probable, that the object or a part of it is under a layer of sediments.

## 6.4 Anomaly AM-04

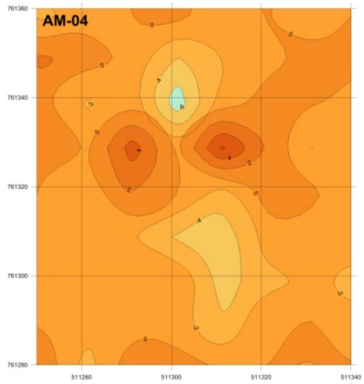


*Fig. 6.8. Enlarged map of the magnetic anomalies showing the anomaly AM-04 in detail*

The figure above (Fig. 6.8.) presents a detailed distribution of the magnetic field for the anomaly AM-04. Values recorded by the sensor and spatial distribution of contour lines on the map indicates the presence of a small ferromagnetic object in this region.

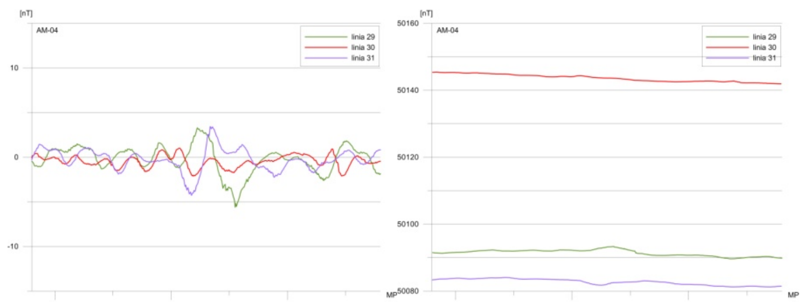


*Fig. 6.9. Charts of magnetic field intensity recorded by the measuring device on three adjoining measuring profiles at the site of the anomaly AM-04*

The figures (Fig. 6.9.) present the charts of a detailed magnetic field intensity distribution for the raw data recorded by the magnetometer on the measuring profiles *29 (the blue colour), 30 (the red colour), 31 (the green colour).* The charts on the right side represent the same data after the filtering process. The values of the magnetic field in this region are characterized by high variability. What's more, there are visible local elevations of the magnetic field at two adjoining profiles. Analysis of the graphs indicates a great impact of the bottom structure on the magnetic field in this region. However, the presence of small ferromagnetic object may not be excluded, for example under the layer of sediments or between measuring profiles.

## 6.5 Anomaly AM-05

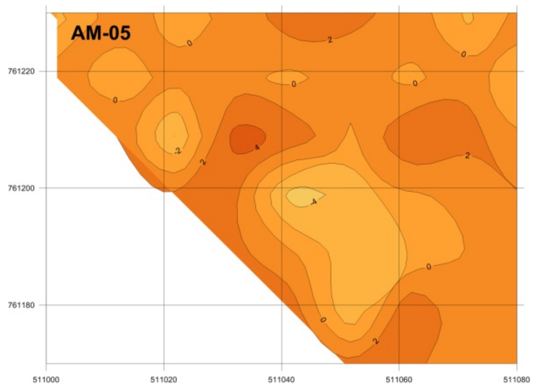


*Fig. 6.10. Enlarged map of the magnetic anomalies showing the anomaly AM-05 in detail*

The figure above (Fig. 6.10.) presents a detailed distribution of the magnetic field for the anomaly AM-05. Values recorded by the sensor and spatial distribution of contour lines on the map indicate the presence of a small ferromagnetic object in this region.

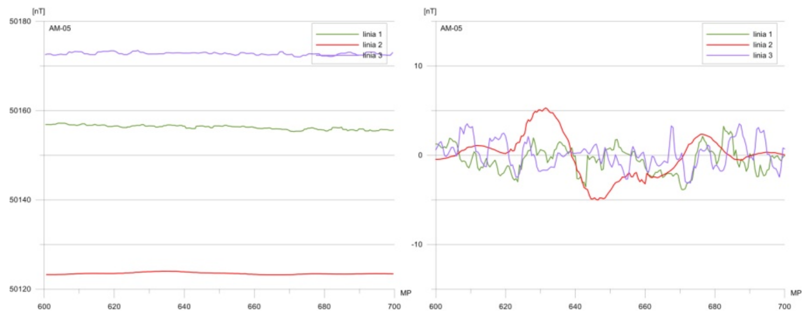


*Fig. 6.11. Charts of magnetic field intensity recorded by the measuring device on three adjoining measuring profiles at the site of anomaly AM-05*

The figures (Fig. 6.11.) present charts of a detailed magnetic field intensity distribution for the raw data recorded by the magnetometer on the measuring profiles *1 (the blue colour), 2 (the red colour), 3 (the green colour).* The charts on the right side represent the same data after the filtering process. The values of the magnetic field in this region are characterized by high variability. What's more, there are visible local elevations of the magnetic field at two adjoining profiles. Analysis of the graphs indicates a greate impact of the bottom structure on the magnetic field in this region. However, the presence of small ferromagnetic object may not be excluded, for example under the layer of sediments or between measuring profiles.

## 6.6 Anomaly AM-06

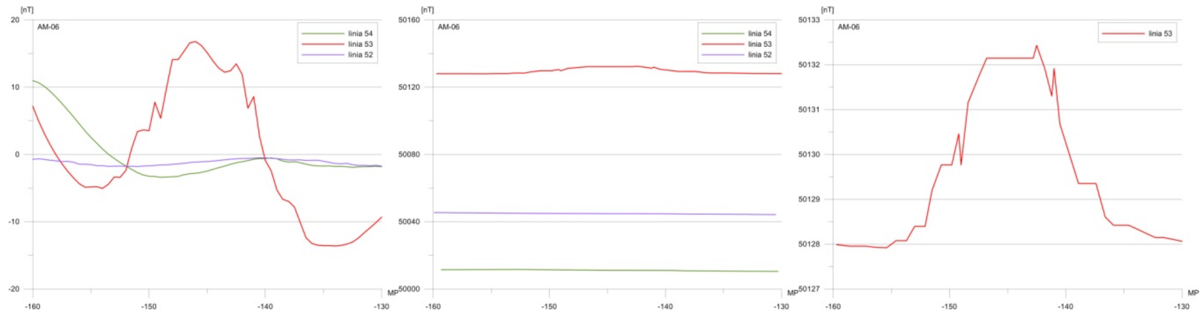


*Fig. 6.12. Charts of magnetic field intensity recorded by the measuring device on three adjoining measuring profiles at the site of anomaly AM-06*

The figures above (Fig. 6.12.) present the magnetic field intensity recorded by the measuring device on three adjoining measuring profiles at the place of occurrence of anomaly AM-06. The anomaly is located outside the area designated for research. On the profile 53, there is visible a clear magnetic anomaly of the value of 15 nT after the filtering and normalization process. The value recorded for the raw data is about 4 nT, which may indicate the presence of a ferromagnetic object in this region. There have not been recorded any increased magnetic field intensity on the adjoining measuring profiles. The shape of the graph indicates a relatively small distance between the measuring device and object during the signal recording. It is also probable that the object or a part of it is under a layer of sediment.

# 7 Conclusions

There have been detected 5 magnetic anomalies in the area of research, plus one more outside the region designated by PNA, which indicate the presence of ferromagnetic objects in this extent.

Not all locations pointed by PNA as places of potential ferromagnetic object presence were the actual span of occurrence of the magnetic anomalies. It is probable, that the specified objects detected with the side scan sonar are objects with no magnetic properties, such as shipwrecks (or parts of wrecks) made of wood.

There is a significant probability, that some of the identified anomalies do not indicate the actual place of ferromagnetic objects deposition. The applied processing technique used to find small magnetic anomalies, involved the deep processing of recorded raw data, and may (in certain situations) lead to errors due to the formation of “nodes”, where the sum of the errors contributes to form “false” objects. However, the places where the positive dipoles are shown next to the negative dipoles may be considered as highly reliable.

Due to the low mass of searched objects the signal recorded by the measuring device was deliberately amplified in order to enhance local anomalies. The values shown in the diagrams are higher in relation to the actual values. However, this method allows to determine the places of the slightly increased values of the magnetic field in the area.

# 8 Literature

Camidge K., Holt P., Johns Ch., Randall L., Schmidt A., *Developing magnetometer techniques to identify submerged archeological sites*, Cornwall 2010.

Gajewski L. and others: *Identyfikacja antropogenicznych obiektów dna morskiego metodami bezinwazyjnymi (sprawozdanie merytoryczne)*, Instytut Morski w Gdańsku, WW 5928, Gdańsk 2002.